IL NUOVO CIMENTO Vol. 26 C, N. 3 Maggio-Giugno 2003

Modeling turbulence perturbation in a laboratory boundary layer flow over hills(*)

M. Antonelli(1) and F. Tampieri(2)

(1) *CNR-ISAC - 40129 Bologna*
(2) *INFM-Departimento di Fisica, Università di Genova - I-16146 Genova*

(ricevuto il 25 Luglio 2002; approvato l'11 Giugno 2003)

Summary. — A second-order closure was used to investigate the effect of a gentle slope hill on the second moments of velocity. An approximated equation system was solved in streamlines coordinates and the mean flow was obtained by means of a linearized model. Results are tested on a very rich data set of two experiments with different slopes.

PACS 92.60.Ek – Convection, turbulence, and diffusion.
PACS 92.60.Fm – Boundary layer structure and processes.
PACS 47.85.-g – Applied fluid mechanics.

1. – Introduction

The atmospheric boundary layer (ABL) turbulence deserves a large attention both as a typical case of shear flow, often affected by density effects, and for the many environmental applications, like evaluation of the effects on buildings and structures, wind energy assessment, pollution dispersion modeling.

A large amount of work has been made to understand and quantitatively describe the structure of ABL turbulence under conditions of horizontal homogeneity; the case of spatial variations of the surface conditions still requires to be investigated also because of its practical importance. In this work we shall address the problem of turbulence perturbations, in the outer region of the ABL, induced by the presence of a gentle slope hill. With the word *outer* we mean here that part of the ABL where the perturbations induced in the flow are essentially inviscid, although the unperturbed ABL itself is driven by turbulent transfer (namely, the unperturbed mean velocity profile is logarithmic under neutral conditions). Typically, the outer region features may be recognised from a few meters above the hill surface. This perturbed region extends up to heights of the order of the horizontal scale length of the hill.

(*) The authors of this paper have agreed to not receive the proofs for correction.

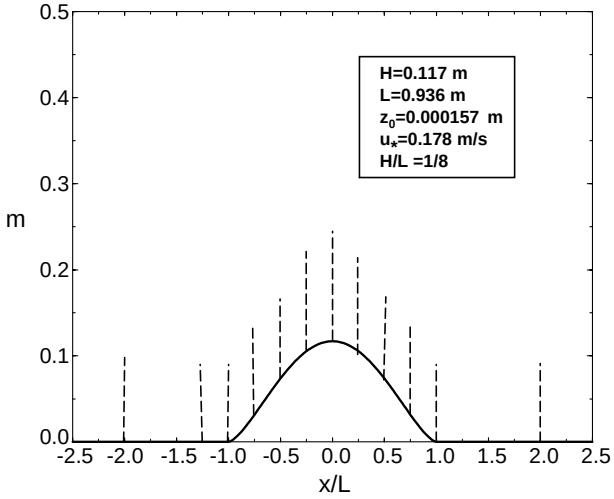

Fig. 1. – The shape of the obstacle in the Rushil H8 experiment and the position of the measures (vertical dashed lines).

The mean flow of the entire ABL over gentle slope hills is well described by linearized models (see [1-3]). The turbulence modifications have been investigated at first by Britter *et al.* [4], and are currently modelled using higher-order closure approaches, as done by Anfossi *et al.* [5, 6, 2, 7]. Since Britter *et al.* [4] work, it is recognised that in the outer region the perturbations affect the larger scale vortices through a distortion mechanism described by the rapid distortion theory (RDT: see [8-10]), whereas the smaller ones are influenced by eddy transport of momentum (see [11]). Accordingly, the seminal paper by Zeeman and Jensen [12] interpreted the turbulence modifications measured over Askervein Hill by a Reynolds stress model based on RDT.

In this paper we shall apply the RTD approach as a diagnostic tool for investigating a wind tunnel experiment of flow over a two-dimensional hill. The experimental data are described by Snyder *et al.* [13] and are known as RUSHIL data (see also [14]). A short description of the experiment and of the relevant data is reported in sect. **2**. The linearized two-dimensional solution for the the mean flow in the outer region is compared with the data in sect. **3**. From this solution, the mean streamlines are derived, and the solution of the equation system governing the Reynolds stresses are computed on the streamline coordinate system, which represents the more natural way to deal with the steady problem, according to Finnigan [15]. This system will be presented and discussed in sect. **4**, whereas in sect. **5** the results obtained are compared with the data.

2. – The data

Very detailed measurements of turbulence characteristics over complex terrain are rarely available in the field. Wind tunnel experiments may provide useful information and test cases for analysing most of the aspects of the problem.

The RUSHIL experiment [13] was designed to investigate in detail the boundary layer perturbations induced by two-dimensional hills, of fixed height $H = 0.117$ m and different slopes. In this paper we shall consider the so-called H8 and H5 hills with half length (at

the basis) $L = 8H$ and $L = 5H$, respectively. The shape of the hill is described by the parametric relation

$$x(\zeta) = \frac{1}{2}\zeta\left[1 + \frac{L^2}{\zeta^2 + m^2(L^2 - \zeta^2)}\right], \tag{1}$$

$$\tilde{f}(\zeta) = \frac{1}{2}m(L^2 - \zeta^2)^{1/2}\left[1 - \frac{L^2}{\zeta^2 + m^2(L^2 - \zeta^2)}\right] \qquad \text{for} \quad |\zeta| \le L\,, \tag{2}$$

$$\tilde{f}(\zeta) = 0\,, \qquad |\zeta| > L\,,$$

$$m = \frac{H}{L} + \left[\left(\frac{H}{L}\right)^{1/2} + 1\right]^{1/2}.$$

In the following numerical computation, we shall need the shape *f(x)* computed on a regular grid. This result is obtained by linear interpolation after computing $(x, \tilde{f})$ pairs for a large number of ζ values.

The shape of the hill and the basic nomenclature is reported in fig. 1.

The EPA wind tunnel was set in order to produce a neutrally stratified BL about 1 m thick, with logarithmic wind profile characterised by $u_* = 0.178$ m/s and $z_0 = 0.157$ mm, leading to a free-stream velocity of 4 m/s. The vertical profiles of mean (U, W), variances ($\overline{u^2}$, $\overline{w^2}$) and covariance ($\overline{uw}$) of the velocity are measured in 15 position from 2L upwind the hilltop to 5L downwind. Hereafter, the vector velocity will be indicated as $(U + u, v, W + w)$ according to the usual Reynolds decomposition. The absolute error ΔU is about 0.05 m/s; the relative error on the second moments is about 10 % (see [13]). Measurements in different positions along the wind tunnel without the hill are also available, and allow to estimate the turbulence decay and more generally the intrinsic inhomogeneity of this BL. Broadly speaking, the second-order moments decay on a distance of about 5 m of 25 %. On the distances investigated in this work (less than 2 m) this decay results of the same magnitude or smaller than the estimated error and this will be neglected in the model-data comparison.

3. – The mean flow

Jackson and Hunt [16] identified a scale of height, l, which is the thickness of the surface layer where the eddy transfer affects the flow perturbations. At greater height, namely in the outer region, the perturbations are essentially inviscid. Such scale is defined by

$$\frac{l}{L}\ln\left(\frac{l}{z_0}\right) = k^2\,. \tag{3}$$

Later authors [2] suggested a different expression for l, which gives a smaller value. We note that this is perhaps of practical relevance but does not affect the physical meaning of this scale.

In the inviscid outer region, the linearization of the Reynolds equations, for the two-dimensional case, leads to the Scorer equation [17], that in the absence of stratification reads

$$\left(\nabla^2 - \frac{U_{zz}}{U}\right)W = 0\,, \tag{4}$$

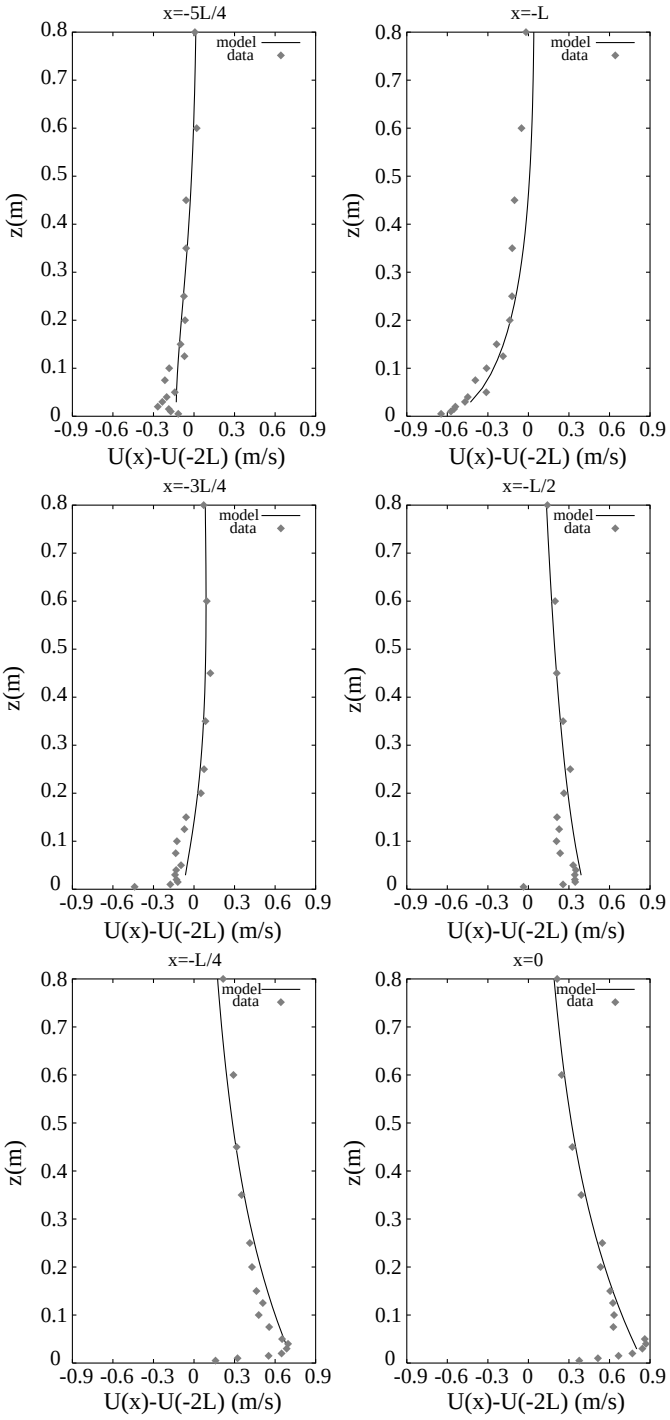

Fig. 2. – Perturbation of the mean velocity with respect to the upstream flow ($U(x = -2L)$) for the H8 experiment calculated by the model (line) and derived from the data (points) in some different positions.

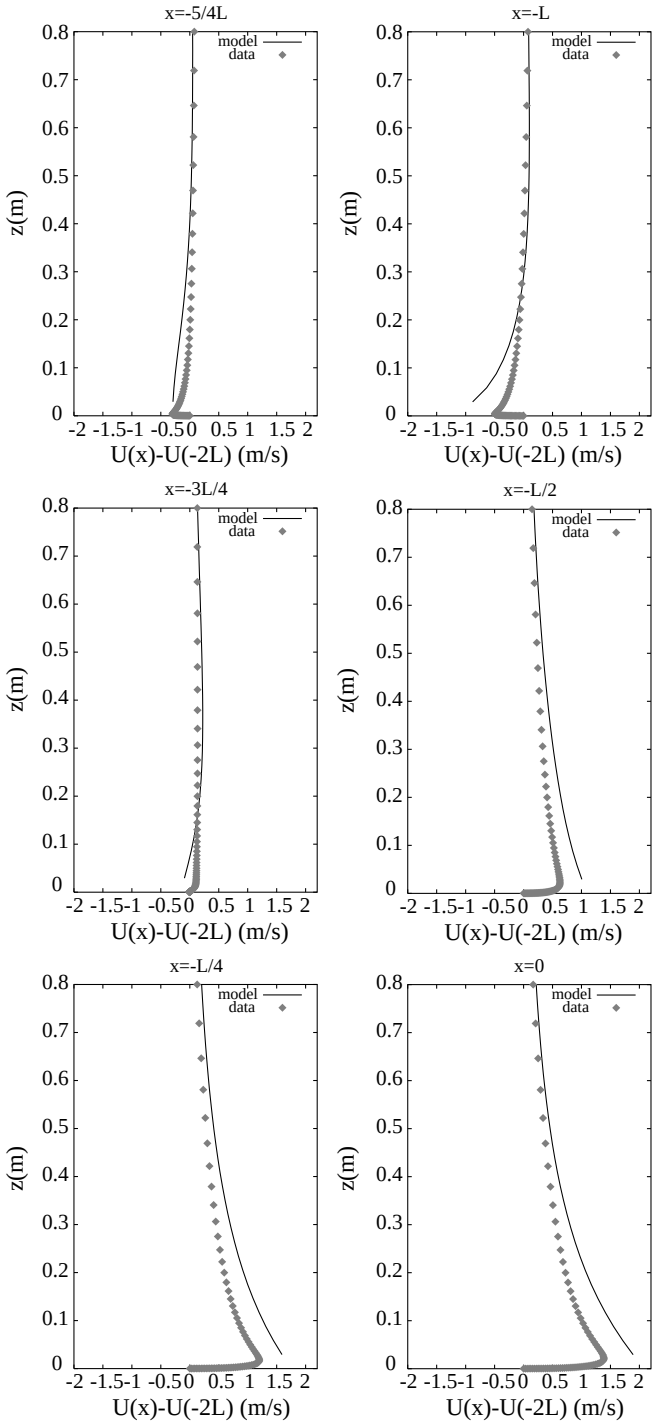

Fig. 3. – Perturbation of the mean velocity with respect to the upstream flow ($U(x = -2L)$) for the H5 experiment calculated by the model (line) and derived from the data (points) in some different positions.

where

$$\nabla^2 = \partial_x^2 + \partial_z^2 \,. \tag{5}$$

It is worth remembering that the linear theory is valid for "gentle slope" hills, that is for obstacles with $H/L \leq 0.5$.

Neglecting the shear term U_{zz}/U we obtain the potential flow solution

$$\begin{aligned} U &= U_0(z) + \frac{H}{L} U_0(L) F^{-1}(\hat{U}) \,, \\ W &= \frac{h}{L} U_0(L) F^{-1}(\hat{W}) \,, \end{aligned} \tag{6}$$

where

$$U_0(z) = \frac{u_*}{\kappa} \ln \frac{z}{z_0} \tag{7}$$

and

$$\hat{U} = |k| \hat{f} e^{-|k|z} \,, \tag{8}$$

$$\hat{W} = ik \hat{f} e^{-|k|z} \,. \tag{9}$$

Here F is the Fourier transform operator, so that, for instance,

$$\hat{f} = F(f) = \frac{1}{2\pi} \int_{-\infty}^{+\infty} f(x) e^{-kx} \mathrm{d}x \tag{10}$$

is the Fourier transform of the topographic shape.

Hunt *et al.* [1] suggested that the solution turns out to be valid for

$$z > h_m = L \frac{1}{\sqrt{\ln(L/z_0)}} \,, \tag{11}$$

where h_m represents the depth of a middle layer, that is inviscid but dominated by the shear effect. By comparing the order of magnitude of the terms (at given height h) in eq. (4) $\partial_x^2 \sim 1/L^2$ and $\frac{U_{zz}}{U} \sim \frac{u_*}{\kappa h^2 U(h)}$ it results they are comparable if $\frac{L^2}{h^2 \ln(h/z_0)} \sim 1$, which is an implicit equation defining h (an estimate of middle layer depth). The height h_m given by eq. (11) is a slight understimate h. In the RUSHIL wind tunnel experiment the ticknesses of the inner and middle layer result:

$$\begin{aligned} l &\sim 0.05\,\mathrm{m} \,, \\ h_m &\sim 0.32\,\mathrm{m} \,, \end{aligned}$$

for $L = 8H$ and

$$\begin{aligned} l &\sim 0.03\,\mathrm{m} \,, \\ h_m &\sim 0.20\,\mathrm{m} \end{aligned}$$

for $L = 5H$.

For the sake of comparison, figs. 2 and 3 show the perturbations to the basic flow derived from the data and those estimated from eq. (6), using the shape defined by eq. (1), for some positions at different distances from the hill top ($x = 0$). The computations are shown from $z = l$ up to $z \sim 8H$. The model shows good agreement with the observations in the entire outer region ($z > h_m$) and in the middle layer too ($l < z < h_m$), in particular upstream of the hill top. Downstream, on the other hand, especially at low heights we have a worse agreement because of the turbulent wake effect which extends at heights greater than l, and that this linear model cannot reproduce.

Thus it appears justified to assume that the mean flow field is well represented by the inviscid linear solution, allowing in particular to compute the streamlines, necessary for the application of the turbulence model, at least in the upstream part of the domain.

4. – The turbulence model in the streamline coordinate system

Streamlines represent in a steady flow the trajectories of fluid particles, so that the streamline coordinate system appears to be the most appropriate to describe the dynamics of turbulence transformation mainly due to vortex deformation (due to the mean flow inhomogeneities) as occurs in the outer region.

The coordinate transformation from the standard Cartesian system (x, z) to the streamline coordinate system (ψ, ϕ) has been widely described by Finnigan [15] and Maurizi *et al.* [18] and is expressed by the following relationships:

$$\frac{\partial \psi}{\partial x} = -W\,, \qquad \frac{\partial \phi}{\partial z} = U\,, \tag{12}$$

$$\frac{\partial \psi}{\partial x} = \zeta U\,, \qquad \frac{\partial \phi}{\partial z} = \zeta W\,, \tag{13}$$

where ζ is an integrating factor. We also define the vorticity $\Omega = \partial U/\partial z - \partial W/\partial x$ in the Cartesian coordinate system. Being a scalar in this 2D model, Ω is invariant with respect to the change of coordinates.

Finnigan [15] wrote the Reynods equations in the streamline coordinate system; they were used by Zeeman and Jensen [12] to model turbulence over Askervein hill and by Maurizi *et al.* [19] to interpret the turbulence balance in the RUSHIL (and the companion RUSVAL [20]) wind tunnel experiments.

The Reynolds equations for a two-dimensional neutrally stratified flow, in this new

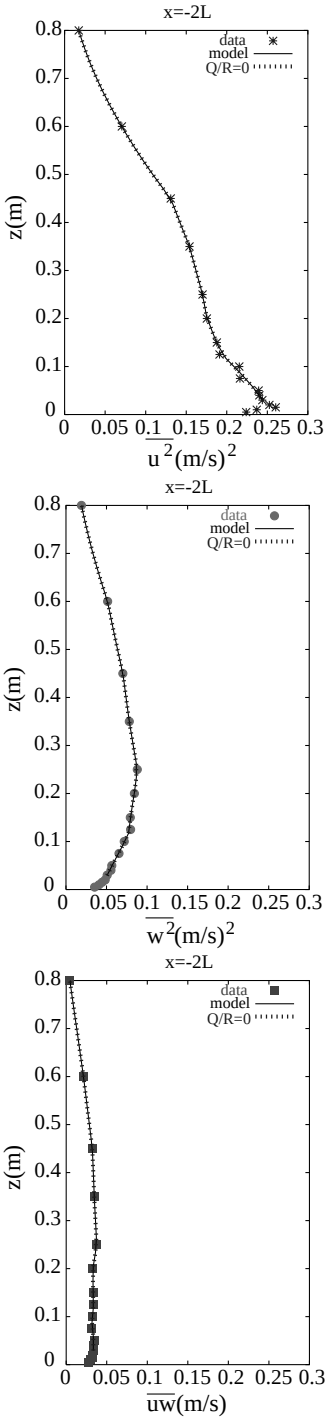

Fig. 4. – Initial profiles ($x = -2L$) of the second-order moments for the H8 experiment.

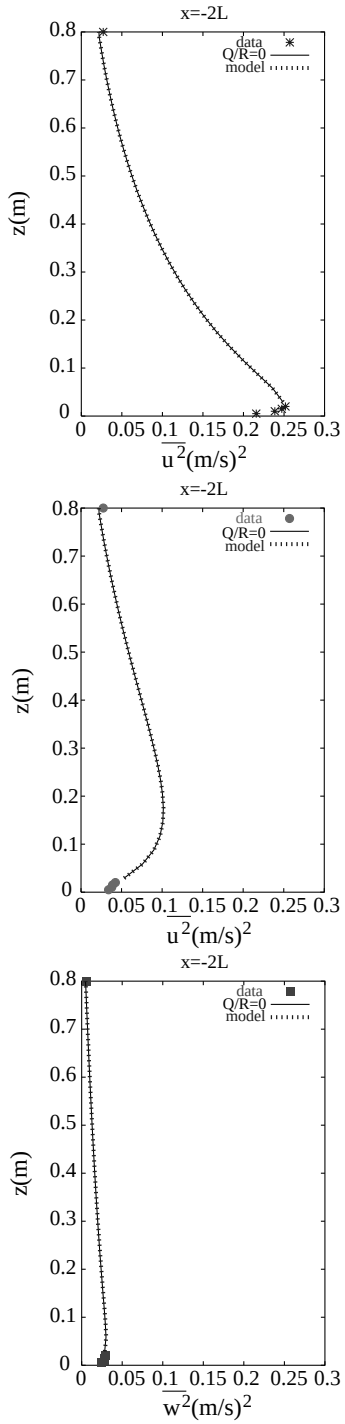

Fig. 5. – Initial profiles ($x = -2L$) of the second-order moments for the H5 experiment.

coordinate system, read

$$U\frac{\partial\overline{u^2}}{\partial x} = -2\overline{u^2}\frac{\partial U}{\partial x} + 2\overline{uw}\frac{U}{R} - 2\overline{uw}\frac{\partial U}{\partial z} - \pi_{11} - \frac{2}{3}\epsilon\,, \tag{14}$$

$$U\frac{\partial\overline{v^2}}{\partial x} = -\pi_{22} - \frac{2}{3}\epsilon\,, \tag{15}$$

$$U\frac{\partial\overline{w^2}}{\partial x} = +2\overline{u^2}\frac{\partial U}{\partial x} - 4\overline{uw}\frac{U}{R} - \pi_{33} - \frac{2}{3}\epsilon\,, \tag{16}$$

$$U\frac{\partial\overline{uw}}{\partial x} = -\overline{w^2}\frac{\partial U}{\partial z} + (\overline{w^2} - 2\overline{u^2})\frac{U}{R} - \pi_{13}\,, \tag{17}$$

where, from now on, x and z are, respectively, the coordinates along a streamline and normal to it, π_{ij} are the so-called pressure terms, ϵ is the dissipation and the radius of curvature R of the $\psi = \text{const}$ lines appears explicitly:

$$\frac{1}{R} = \frac{1}{U}\Big(\Omega + \frac{\partial U}{\partial z}\Big)\,. \tag{18}$$

Note that in this system $W = 0$, so mean advection is only described by the horizontal component U.

In the equations the gradients of $\overline{u_i u_j u_k}$ have been neglected, consistently with the assumption of negligible turbulent transport of momentum in the outer region. An order of magnitude evaluation of the terms gives

$$\begin{cases} \dfrac{\partial\overline{u_i u_j u_k}}{\partial z} \sim O\left(\dfrac{u_*^3}{z}\right)\,, \\ U\dfrac{\partial\overline{u_i u_j}}{\partial x} \sim O\left(U_0\dfrac{u_*^2}{L}\right)\,, \end{cases} \tag{19}$$

thus

$$\frac{\partial\overline{u_i u_j u_k}}{\partial z} \ll U\frac{\partial\overline{u_i u_j}}{\partial x}\,, \qquad \text{if} \qquad z \gg \overline{l}\,,$$

where

$$\frac{\overline{l}}{L}\ln\frac{\overline{l}}{z_0} \sim k\,. \tag{20}$$

A comparison between eq. (20) and eq. (3) shows that the height $\overline{l}$ over which the third-order gradients become negligible with respect to the advection term is $\overline{l} \sim l$, consistently with the hypothesis made about the inviscid outer region dynamics.

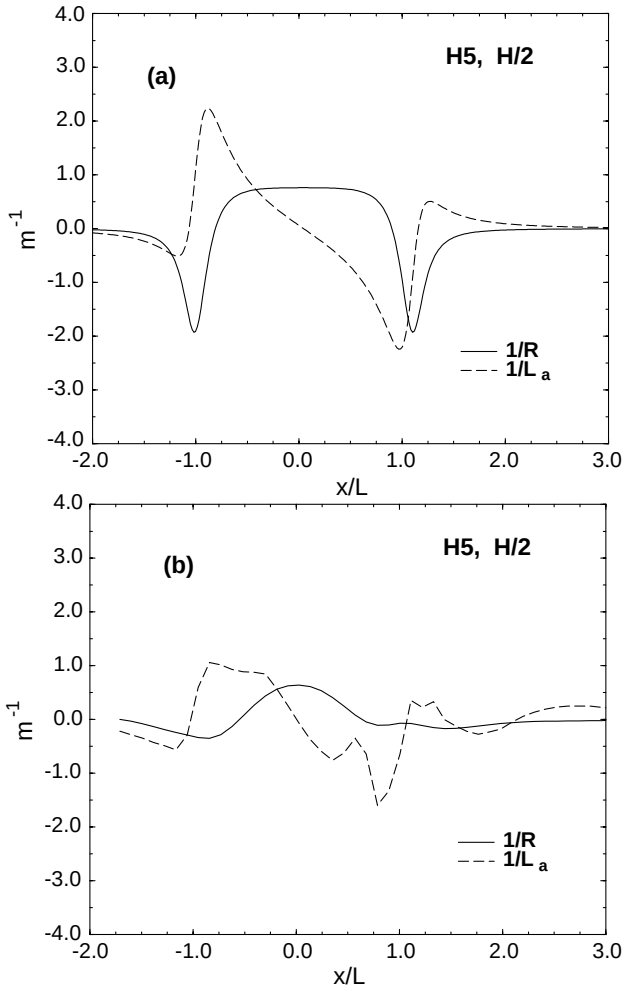

Fig. 6. – The two figures show a comparison of the streamwise acceleration ($1/L_a$) and the inverse of curvature ($1/R$) obtained by the model (a) and recostructed by data of Rushil experiment (b).

Moreover, those terms have been evaluated as residuals in the analysis of turbulent budget over a model valley in the same wind tunnel [19]. It results that the parameterization of third-order moments with a typical flux-gradient model provides a worse description than a model which neglects third-order moments.

The pressure terms can be rewritten according to the model by Zeman and Tennekes [21] as

$$\pi_{ij} = \pi_{ij}^R + \pi_{ij}^D \,, \tag{21}$$

where

$$\pi_{ij}^R = Cq^2 b_{ij} \qquad \left(b_{ij} = \frac{\overline{u_i u_j}}{q^2} - \delta_{ij} \right) \tag{22}$$

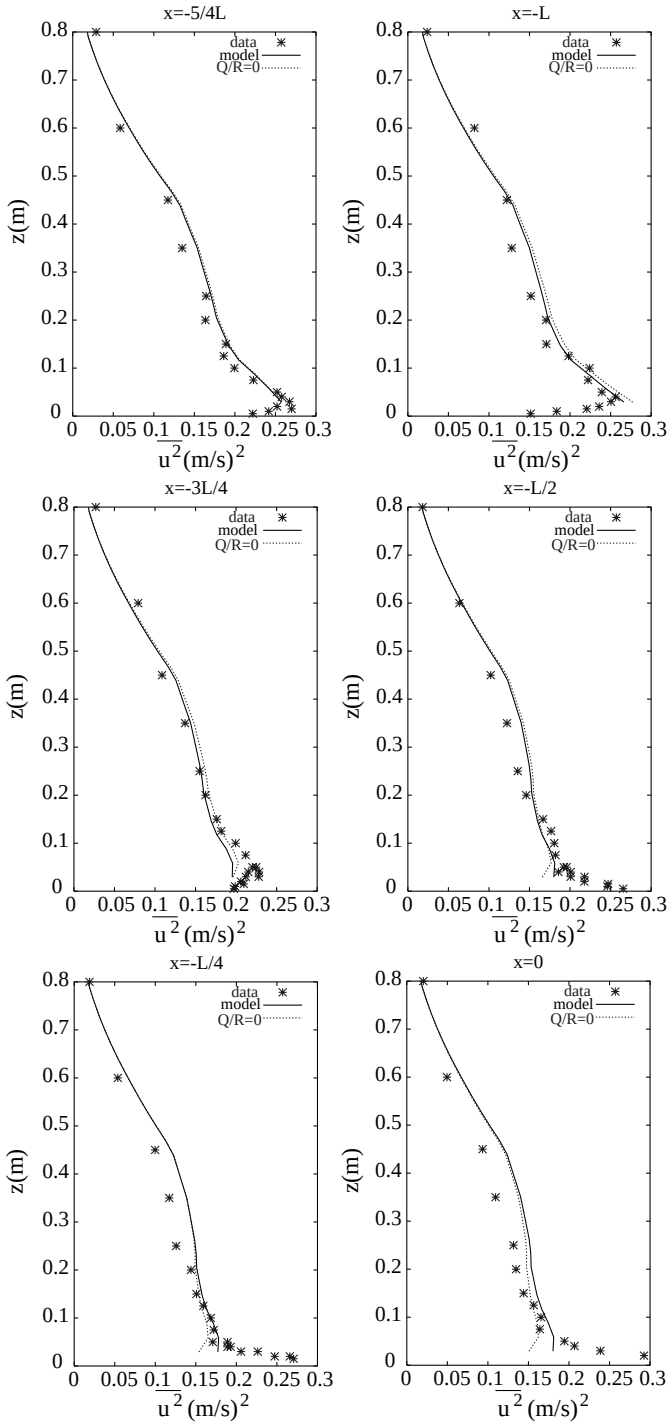

Fig. 7. – Vertical profiles of $\overline{u^2}$ in some different positions for H8 experiment. The data (stars) are compared with the model which includes the curvature effect (solid line) and the model without curvature effect (pointed line).

is Rotta's term which describes the return to isotropy, and

$$\pi_{11}^D = -\frac{\partial U}{\partial x}\left[\frac{2}{5}q^2 + \frac{4}{3}\alpha_1(\overline{u^2} - \overline{v^2})\right] - 2\frac{\partial U}{\partial z}\overline{uw}(\alpha_1/3 + \alpha_2) - \tag{23}$$
$$-2\frac{U}{R}\overline{uw}(\alpha_1/3 - \alpha_2)\,,$$

$$\pi_{22}^D = -\frac{\partial U}{\partial x}\frac{4}{3}\alpha_1(\overline{u^2} - \overline{w^2}) + \frac{\partial U}{\partial z}\frac{4}{3}\alpha_1\overline{uw} + \frac{U}{R}\frac{4}{3}\alpha_1\overline{uw}\,, \tag{24}$$

$$\pi_{33}^D = -\frac{\partial U}{\partial x}\left[\frac{2}{5}q^2 + \frac{4}{3}\alpha_1(\overline{w^2} - \overline{v^2})\right] - 2\frac{\partial U}{\partial z}\overline{uw}(\alpha_1/3 - \alpha_2) - \tag{25}$$
$$-2\frac{U}{R}\overline{uw}(\alpha_1/3 + \alpha_2)\,,$$

$$\pi_{13}^D = -\frac{\partial U}{\partial z}\left[\frac{1}{5}q^2 + \alpha_1\left(\overline{w^2} + \overline{u^2} - \frac{2}{3}q^2\right) + \alpha_2(\overline{w^2} - \overline{u^2})\right] - \tag{26}$$
$$-\frac{U}{R}\left[\frac{1}{5}q^2 + \alpha_1\left(\overline{w^2} - \overline{u^2} - \frac{2}{3}q^2\right) + \alpha_2(\overline{u^2} - \overline{w^2})\right]$$

are the so-called *rapid distortion* term in the streamline coordinate system; $(1/2)q^2$ is the turbulent kinetic energy and α_1, α_2 and C are constants to be determined from the data. This closure results from the application of the RDT. The RDT approximation corresponds, in the present problem, to limit the description to cases for which the typical integral time scale of eddies (which is a measure of nonlinear interaction time among eddies) $T_t = kz/u_*$ is larger than the mean flow distortion time $T_D = U/L$:

$$T_D \ll T_t \Rightarrow \frac{L}{\frac{u_*}{k}\ln(z/z_0)} \ll \frac{kz}{u_*}\,, \tag{27}$$

$$\Rightarrow\ \frac{z}{L}\ln\frac{z}{z_0} \ll 1\,, \tag{28}$$

therefore the RDT approximation is valid for $z > l$, that is in the outer region.

The three constants α_1, α_2, C in the pressure term model (eqs. (22)-(26)) can be calculated for each particular partition of turbulent kinetic energy distrubution among the component of the Reynolds stress tensor. From eqs. (14)-(17) applied over flat terrain, using espressions (22)-(26) and assuming a local equilibrium to model the dissipation term as $\epsilon = -\overline{uw}\frac{\partial U}{\partial z}$, we obtain the following equation system with the three unknowns α_1, α_2, C:

$$2\left(1 - \frac{1}{3}\alpha_1 - \alpha_2\right) - b_{11}C - 2/3 = 0\,, \tag{29}$$

$$\frac{4}{3}\alpha_1 - b_{22}C - 2/3 = 0\,, \tag{30}$$

$$-\frac{2}{3}\alpha_1 + 2\alpha_2 - b_{33}C - 2/3 = 0\,, \tag{31}$$

$$-\frac{u_3^2}{u_*^2} - \alpha_2(b_{11} - b_{33})\frac{q^2}{u_*^2} + \frac{1}{5}\frac{q^2}{u_*^2} - \alpha_1 b_{22}\frac{q^2}{u_*^2} + C\frac{u_*^2}{q^2} = 0\,. \tag{32}$$

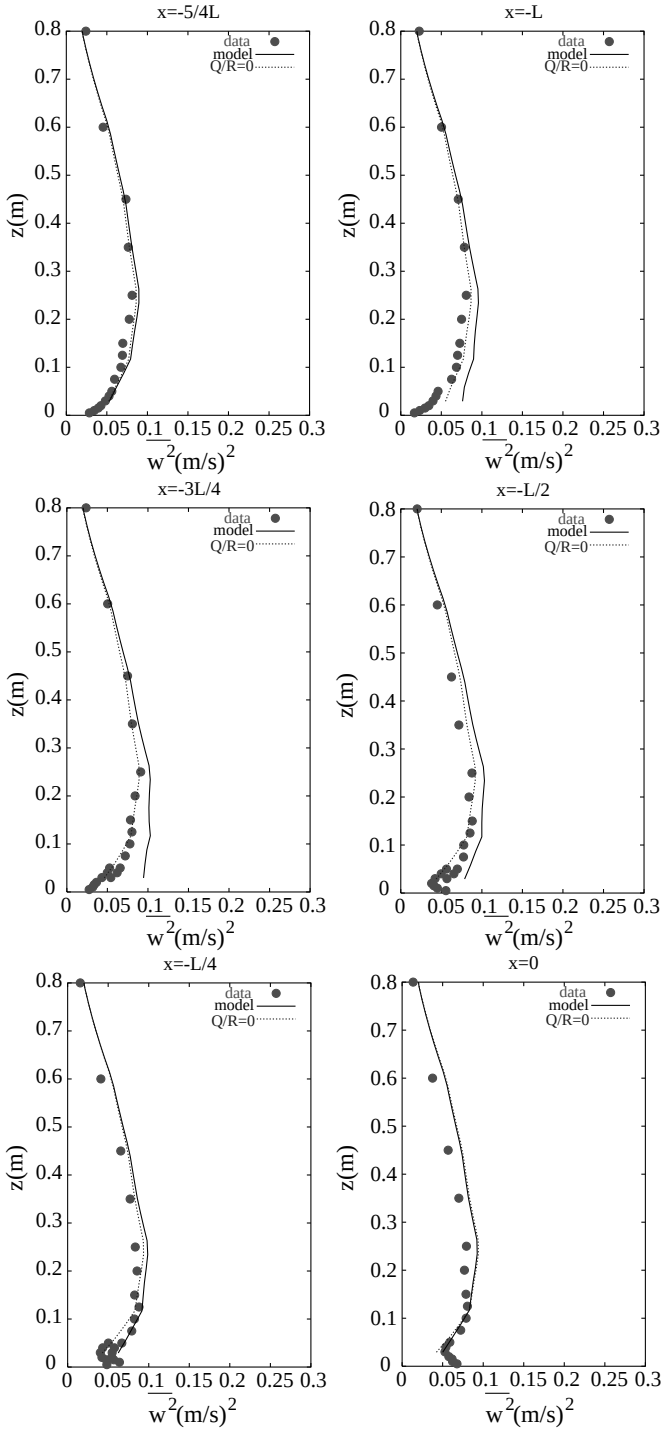

Fig. 8. – The same of fig. 7 for $\overline{w^2}$.

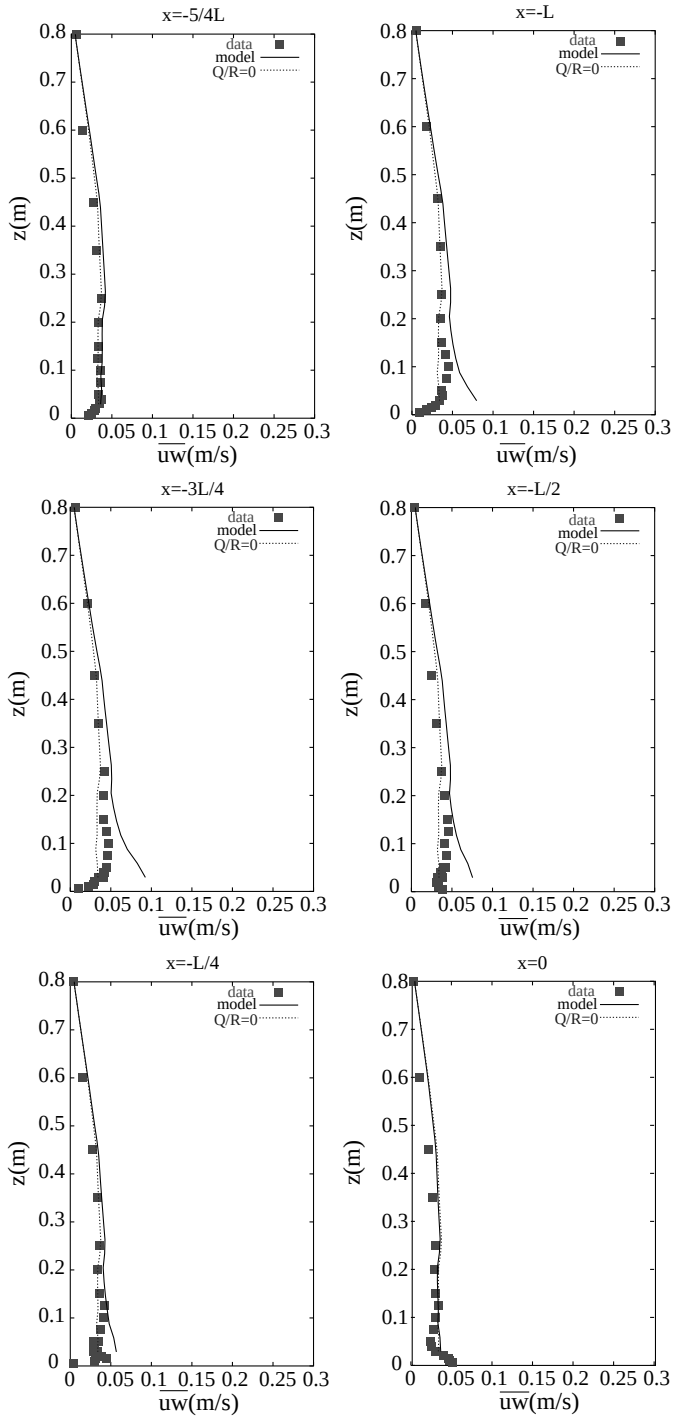

Fig. 9. – The same of fig. 7 and fig. 8 for $\overline{uw}$.

The first three equations are not independent, so that we get a three-equations system with three unknowns:

$$\alpha_1 = \frac{1}{10(b_{11}^2 - \frac{1}{2}b_{22}^2 + b_{11}b_{22} + \frac{u_*^2}{q^2})} + \frac{1}{2}\,, \tag{33}$$

$$\alpha_2 = -\frac{2b_{11} + b_{22}}{30(b_{11}^2 - \frac{1}{2}b_{22}^2 + b_{11}b_{22} + \frac{u_*^2}{q^2})} + \frac{1}{2}\,, \tag{34}$$

$$C = \frac{2/15}{b_{11}^2 - \frac{1}{2}b_{22}^2 + b_{11}b_{22} + \frac{u_*^2}{q^2}}\,. \tag{35}$$

For a given turbulent kinetic energy distribution, that is for each tern of values of u_1^2/q^2, u_2^2/q^2 and u_*^2/q^2, it is possible to calculate the corresponding values of the constants of the model. Since the values of u_i^2 are not constant with height (see fig. 4), the constants of the model are calculated for each streamline assuming a local equilibrium which changes with height.

In the present formulation the equations describing the Reynolds stresses dynamics are ordinary differential equations instead of partial differential equations. This system has been integrated along streamlines at different heights $z_n = nH/4$ using a Runge-Kutta method of fourth order. We integrated the equations from the position $x = -2L$ using as initial value for u_i^2 the experimental data in the same point (figs. 4, 5).

Although these profiles are far from ideal (in fact they show an inflection at $z \sim 3h$) they give the true initial condition for the present problem, and the discussion will concentrate on the evolution for $x > -2L$, mainly due to the presence of the obstacle.

For experiment H5 we do not have a detailed profile for u_i^2 in $x = -2L$ but only a reconstruction from a few data near the ground and at the top of the boundary layer.

The experiments H5 and H8 do not provide measures of $\overline{v^2}$ so that we use a value typical of the neutral boundary layer [22], $v^2/-\overline{uw} = 3.24$.

To evaluate the effects of the mean flow deformation on turbulent stresses we rewrite the system (14)-(17) evidencing the crossflow shear $\partial U/\partial z$ the curvature U/R, and the

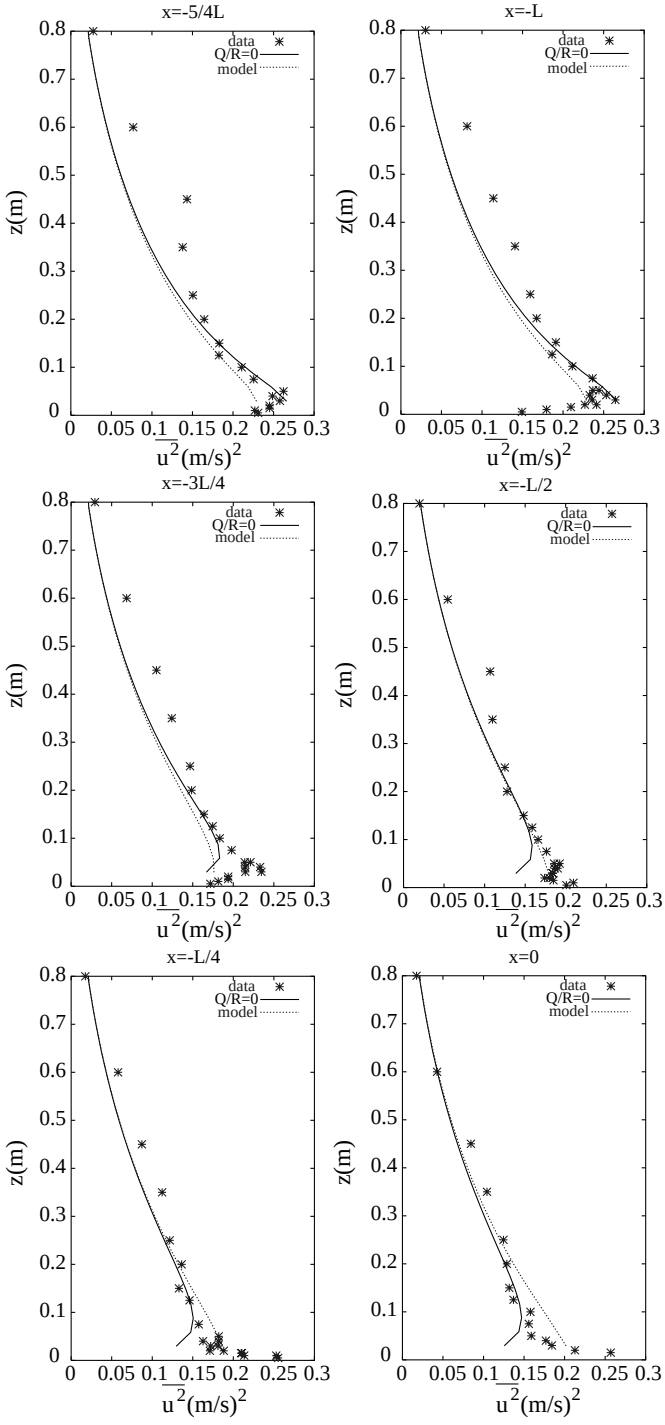

Fig. 10. – Vertical profiles of $\overline{u^2}$ in some different positions for H5 experiment. Data (stars) are compared with the model which includes the curvature effect (solid line) and with the model without curvature (pointed line).

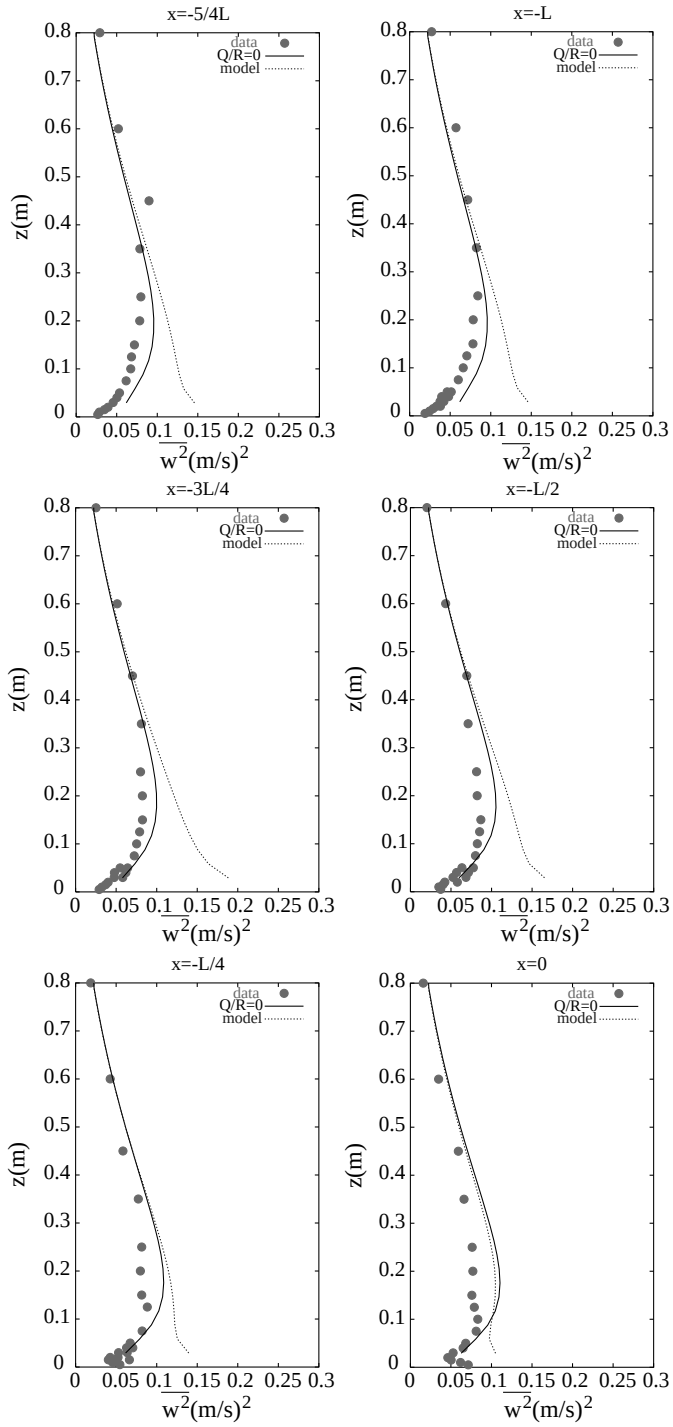

Fig. 11. – The same of fig. 10 for $\overline{w^2}$.

streamwise acceleration $\partial U/\partial x$:

$$(36)\quad U\frac{\partial\overline{u^2}}{\partial x} = \frac{\partial U}{\partial x}\left[-2\overline{u^2} + 2/5q^2 + 4/3\alpha_1(\overline{u^2} - \overline{v^2})\right] + \\ + \frac{U}{R}(2\overline{uw} + 2\overline{uw}(\alpha_1/3 - \alpha_2)) + \\ + \frac{\partial U}{\partial z}2\overline{uw}(\alpha_1/3 - \alpha_2) - C\epsilon\left(\frac{u^2}{q^2} - \frac{1}{3}\right) - \frac{2}{3}\epsilon\,,$$

$$(37)\quad U\frac{\partial\overline{v^2}}{\partial x} = \frac{\partial U}{\partial x}4/3\alpha_1(\overline{u^2} - \overline{v^2}) - \frac{U}{R}4/3\alpha_1\overline{uw} - \frac{\partial U}{\partial z}4/3\alpha_1\overline{uw} - \\ - C\epsilon\left(\frac{v^2}{q^2} - \frac{1}{3}\right) - \frac{2}{3}\epsilon\,,$$

$$(38)\quad U\frac{\partial\overline{w^2}}{\partial x} = \frac{\partial U}{\partial x}\left[2\overline{u^2} + 2/5q^2 + 4/3\alpha_1(\overline{w^2} - \overline{v^2})\right] + \\ + \frac{U}{R}(-4\overline{uw} + 2\overline{uw}(\alpha_1/3 + \alpha_2)) + \\ + \frac{\partial U}{\partial z}(2\overline{uw}(\alpha_1/3 - \alpha_2)) - C\epsilon\left(\frac{w^2}{q^2} - \frac{1}{3}\right) - \frac{2}{3}\epsilon\,,$$

$$(39)\quad U\frac{\partial\overline{uw}}{\partial x} = \frac{U}{R}\left[\overline{w^2} - 2\overline{u^2} + \frac{1}{5}q^2 + \alpha_1\left(\overline{w^2} - \overline{u^2} - \frac{2}{3}q^2\right) + \alpha_2(\overline{u^2} - 2\overline{w^2})\right] + \\ + \frac{\partial U}{\partial z}\left[-\overline{w^2} + \frac{1}{5}q^2 + \alpha_1\left(\overline{w^2} + \overline{u^2} - \frac{2}{3}q^2\right) + \alpha_2(\overline{w^2} - 2\overline{u^2})\right] - C\epsilon\frac{u^2}{q^2}\,.$$

The equation for $-\overline{uw}$ (eq. (39)) has the simplest form and can be used to estimate the order of magnitude of the effect of curvature and of the shear.

If one considers typical values of turbulent stresses in the ABL [14] and of the costants α_1 and α_2 [21]

$$(40)\quad \begin{cases} \overline{u^2} = 6.25u_*^2\,, \\ \overline{w^2} = 1.69u_*^2\,, \\ \overline{v^2} = 3.24u_*^2\,, \\ \overline{-uw} = u_*^2\,, \\ \alpha_1 = 0.31\,, \\ \alpha_2 = 0.2\,, \end{cases}$$

we find that

$$(41)\quad U\frac{\partial(-\overline{uw})}{\partial x} = A\frac{\partial U}{\partial z} + B\frac{U}{R}$$

with

$$\begin{cases} A \simeq 0.2 u_*^2 \,, \\ B \simeq 12. u_*^2 \,, \end{cases} \tag{42}$$

while for the along wind variance $\overline{u^2}$ results:

$$U \frac{\partial(\overline{u^2})}{\partial x} = D \frac{\partial U}{\partial x} + E \frac{U}{R} + F \frac{\partial U}{\partial z} \tag{43}$$

with

$$\begin{aligned} D &\simeq -7 u_*^2 \,, \\ E &\simeq -2 u_*^2 \,, \\ F &\simeq -1 u_*^2 \,. \end{aligned}$$

So the curvature effect is the dominant one in the equation for $-\overline{uw}$ and the less important for $\overline{u^2}$.

Since the sign of the curvature is

$$\begin{aligned} &\frac{U}{R} > 0 \qquad \text{in the upwind slope and behind the hill} \\ &\frac{U}{R} < 0 \qquad \text{over the hilltop} \end{aligned}$$

according to Kaimal and Finnigan [23], the effect is to reduce $-\overline{uw}$ and $\overline{w^2}$ on the top and to increase them at the foots of the hill.

The streamlines resulting from the application of the linearized model to compute the mean flow (see sect. **3**) follow the shape of topography more stricly than in the real case because the effect of nonlinearity would be to smooth strong variation of velocity in particular at the hill foot. It results that the model tends to overestimate the streamline curvature as we can see from a comparison (showed in figs. 6a, b) between curvature and streamline of the model and those derived from experimental data [24]. In particular it gives a quite unrealistic negative minimum of curvature at the hill foot, whereas the positive maximum over the hill top is well reproduced.

So it results that the integration of eqs. (14)-(17) with the mean strain rate computed from the linearized model produces a strong positive perturbation for $-\overline{uw}$ and $\overline{w^2}$ which affects the results downstream.

To evaluate the curvature effect, in figs. 7, 8, 9, and figs. 10, 11, 12 we compare the results of the full model with those obtained from the same system putting $U/R = 0$.

From the turbulent stress profiles showed in the figures, it is evident that the full model with the curvature derived from the "linear" mean flow produces an excessive perturbation on $-\overline{uw}$ and $\overline{w^2}$ and this overestimation is advected along the streamlines until the top. The model with $U/R = 0$, on the other hand, produces a correct perturbation at the hill foot, whereas it overestimates these components of the stresses over the hill top. From the analysis of the data it results that the curvature effect is almost negligible at the hill foot, whereas it should reduce $-\overline{uw}$ and $\overline{w^2}$ over the hill top, consequently the net effect over the hill top is a decrease of $-\overline{uw}$ and $\overline{w^2}$.

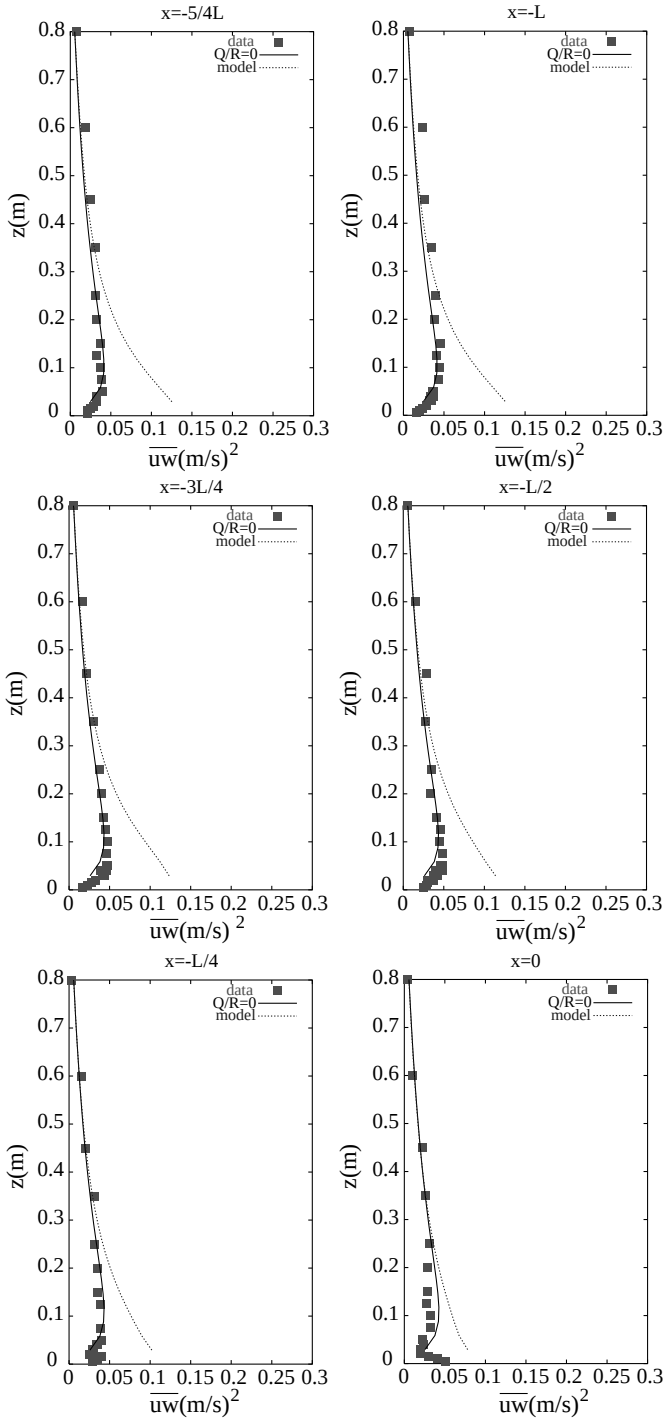

Fig. 12. – The same of fig. 10 and fig. 11 for $\overline{uw}$.

Of course the nonlinear effects and consequently the overestimation of curvature are more evident in the H5 experiment because of its greater slope. Also we can notice that the model reproduces the vertical profiles of $\overline{u^2}$ very well in both the experiments. This is consistent with the fact that the leading term in the equation for $\overline{u^2}$ is the streamwise acceleration $\partial U/\partial x$ (which is well reproduced by the linear model) as is shown in the previous analysis.

5. – Conclusions

In this work we applied a simplified method to solve the equation system for Reynolds stresses over a low hill and we verified its validity over a very rich data set.

We focused our attention on the outer region of the flow, where the eddy viscosity effect can be neglected.

The use of a linearized model for the mean velocity field produces a good description of the mean flow perturbation over the obstacle (as well known from previous works). This mean flow field has been used to compute the streamlines and the derivatives of the mean velocity necessary to compute the Reynold stresses perturbation.

Some perturbation of the Reynolds stresses upwind and over the top are well captured by the model, namely those of the along wind variance ($\overline{u^2}$); whereas others ($\overline{w^2}$ and $\overline{uw}$) are not. From the analysis of the governing equations it results that small inaccuracies, which arise in the mean flow description, can have a large influence on (at least) some components of the Reynold stresses. In particular the error associated to the curvature radius (related to the shape of the obstacle which directly affects the streamline shape as computed by linear model) affect the value of $\overline{w^2}$ and $\overline{uw}$ components at the upwind foot of the hill and propagates up to the hill top.

So a first-order linear model, which well reproduces the perturbation of the mean flow over a gentle slope hill is shown to produce an unrealistic perturbation on the turbulent energy distribution on the top.

REFERENCES

[1] Richards K. J., Hunt J. C. R. and Leibovich S., *Q. J. R. Meteorol. Soc.*, **114** (1988) 435.
[2] Taylor P. A., Mason P. J. and Bradley E. F., *Boundary-Layer Meteorol.*, **39** (1987) 107.
[3] Hunt J. C. R. and Belcher S. E., *Ann. Rev. Fluid Mech.*, **30** (1998) 507.
[4] Richards K. J., Britter R. E. and Hunt J. C. R., *Q. J. R. Meteorol. Soc.*, **107** (1981) 91.
[5] Anfossi D., Ying R., Trini Castelli S. and Ferrero E., *Comparison of turbulence closure models over a schematic valley in a neutral boundary layer*, in *13th Symposium on Boundary Layer and Turbulence-79th Annual Meeting*, 1999.
[6] Pittaluga F., Duranti S. and Pezzuto G., *Wind J. Eng. Ind. Aerodyn.*, **74** (1998) 263.
[7] Ypma R. M., Ying R. and Canuto V. M., *Boundary-Layer Meteorol.*, **70** (1994) 401.
[8] Hunt J. C. R. and Carruthers D. J., *Fluid J. Mech.*, **212** (1990) 497.
[9] Townsend A. A., *The Structure of Turbulent Shear Flows* (Cambridge University Press) 1976.
[10] Scott J. F. and Cambon C., *Ann. Rev. Fluid Mech.*, **31** (1999) 1.
[11] Frank H. P., *Boundary-Layer Meteorol.*, **79** (1996) 345.
[12] Zeman O. and Jensen N. O., *Q. J. R. Meteorol. Soc.*, **113** (1987) 55.

[13] Snyder W. H., Khurshudyan L. H. and Nekrasov I. V., *Flow and dispersion of pollutant within two-dimensional hills*, EPA Report N. 600/4-81/067 (1981).
[14] Tampieri F., Trombetti F. and Martano P., *Data sets for studies of flow and dispersion in complex terrain:I the rushil wind tunnel experiment (flow data)*, Technical paper n.1, Fisbat -CNR, Bologna (Italy), 1991.
[15] Finnigan J. J., *Fluid J. Mech.*, **130** (1983) 241.
[16] Hunt J. C. R. and Jackson P. S., *Q. J. R. Meteorol. Soc.*, **101** (1975) 929.
[17] Scorer R. S., *Dynamics of Meteorology and Climate* (John Wiley and sons, Chichester) 1997.
[18] Trombetti F., Maurizi A. and Di Sabatino S., *Boundary-Layer Meteorol.*, **82** (1997) 379.
[19] Maurizi A., Trombetti F., Di Sabatino S. and Tampieri F., *Reliability of third order moment parameterization for model of turbulent boundary layer over gentle topography*, in *Nuovo Cimento C*, **20** (1997) 273.
[20] Nekrasov I. V., Lawson R. E., Thompson R. S., Khurshudyan L. H., Snyder W. H. and Shiermeier F. A., *Flow and dispersion of pollutant within two-dimensional valleys*, EPA Report N. 600/3-90/025 (1990).
[21] Zeman O. and Tennekes H., *J. Atmos. Sci.*, **32** (1975) 1808.
[22] Trombetti F. and Tagliazucca M., *Characteristic scales of the athmospheric surface layer*, Technical paper n.4, Fisbat -CNR, Bologna (Italy), 1994.
[23] Kaimal J. C. and Finnigan J. J., *Atmospheric Boundary Layer Flows* (Oxford University Press, New York) 1994.
[24] Di Sabatino S., Maurizi A. and Trombetti F., *Data set for studies of flow and dispersion in complex terrain: turbulence futures in streamline coordinates in the RUSHIL and RUSVAL wind tunnel experiments*, Technical paper n.5, Fisbat-CNR, Bologna (Italy), 1995.